A PARK TRANSFORM-BASED METHOD FOR CONDITION MONITORING OF THREE-PHASE ELECTROMECHANICAL SYSTEMS

Christopher Laughman*, Steven B. Leeb†, Leslie K. Norford‡, Steven R. Shaw§ and Peter R. Armstrong¶

*Mitsubishi Electric Research Laboratories
201 Broadway, Cambridge, MA 02139
email: laughman@merl.com

†Department of Electrical Engineering and Computer Science
Massachusetts Institute of Technology, Cambridge, MA 02139
email: sbleeb@mit.edu

‡Department of Architecture
Massachusetts Institute of Technology, Cambridge, MA 02139
email: lnorford@mit.edu

§Department of Electrical and Computer Engineering
Montana State University, Bozeman, MT 59717
email: sshaw@matrix.coe.montana.edu

¶Masdar Institute of Science and Technology, Abu Dhabi, United Arab Emirates
email: parmstrong@masdar.ae

Abstract—This paper presents a Park transform-based method for preprocessing stator current data from a motor and transforming it into a form that is useful for fault detection and diagnostics. The proposed method generates power signatures that are invariant to the initial electrical angle of the voltage when the motor is connected to the utility, and can also adapt to variations in the electrical angle of the supply voltage over time. A modified nonlinear least squares algorithm identifies and tracks the parameters of the supply voltage over time, ensuring that the supply voltage and the argument of the Park transformation remain synchronized. Experimental results are presented that illustrate the method's effectiveness for identifying changes in the mechanical load on a 3/4 HP refrigeration compressor.

I. INTRODUCTION

As the cost of energy rises and electromechanical systems perform a growing share of important functions in our society, methods that assess the reliability of these systems are increasing in importance. Such methods may be designed to enable condition-based or "just-in-time" maintenance. Monitoring systems may assume a range of complexity, from the installation of a simple sensor that produces an alarm when a fault condition is manifested, to a system which monitors and identifies trends in the system state and model parameters which are indicative of either normal or abnormal events or operation. Fully automatic monitoring and control systems may also be used to adjust the system operation by incorporating such information.

Rotating electric machinery is subject to a wide variety of faults at both the electrical and the mechanical ports. Some representative electrical faults include broken rotor bars, shorted windings, and rotor eccentricity. Mechanical faults may also occur, including bearing failure, load imbalance, and other related faults that are associated with the particular load being driven. One popular strategy for identifying these faults involves the sole use of electrical measurements to identify a variety of either electrical or mechanical faults. These methods are appealing because the lack of mechanical sensors may reduces both the cost of fault monitoring and the probability of false alarms due to sensor failures.

Fault diagnosis through electrical monitoring has received a great deal of attention over the last 20 years [1], [11], [15]–[17], and has been successfully used to identify many different electrical and mechanical fault conditions. One particularly popular approach is referred to as motor current signature analysis (MCSA) [4], in which the spectra of the monitored currents are analyzed and coupled with a priori knowledge to identify a number of different faults. These methods have also been extended to monitor other mechanical quantities, such as rotor speed, by only using measurements of the electrical terminal variables [3], [5]. Methods have also been developed which can simultaneously identify both electrical and mechanical parameters of models of the machine, and which can evaluate the condition of the machine from the behavior of these parameters [9], [14].

Condition monitoring methods based upon the analysis of the machine's time domain behavior, such as non-intrusive load monitoring [8], [10] can be quite useful, due to the fact that many different faults evince characteristics that change with time. Such methods can provide a variety of information to an equipment operator or facilities manager, such as power consumption and diagnostic capabilities. Such electrical monitoring techniques are challenging to implement in AC systems for at least two reasons. First, the relevant changes in the stator currents are modulated on top of the base utility frequency (e.g. 60 Hz), so that the waveform must

effectively be demodulated to facilitate the implementation of high-accuracy change detection methods. Second, observations of individual phase currents on multi-phase machines during the transient startup period of the machine are dependent upon both the initial conditions of the system (e.g. initial phase of the utility and the initial position of the rotor and the coupled mechanical system) and the dynamic behavior of the machine. Observations of one current thus may not adequately reveal the possible manifestations of faulty behavior.

The well-known Park or coordinate-frame transformation for three-phase machinery can provide a useful framework for these diagnostics. These rotating transformations are commonly used for machine design and control, but the simplifications that result from applying the transformation can also be useful for condition monitoring [2]. This research examines the application of the synchronously rotating reference frame to diagnostic methods for induction machines in HVAC applications, such as refrigeration compressors.

A principal benefit of this transformation is that the 60 Hz components of the electrical waveforms can be eliminated by synchronizing the transform with the electrical angle of the utility. The resulting transformed waveforms can expose small changes in the machine behavior [10]. The transformation of the observed stator currents will also produce identical results regardless of the starting angle because the initial angle of the utility is incorporated into the transformation matrix.

In an active control application, the rotating frame transformation is relatively easy to implement, because the controller specifies and measures the characteristics of the drive waveforms. The transformation is much more difficult to implement on machines that are connected directly to the electric utility, however, since the characteristics of the utility voltage must be modeled and measured accurately to identify the electrical angle. This becomes especially challenging when the electrical angle of the drive waveforms is not a simple affine function of time.

This paper proposes a method for performing condition monitoring on three-phase electromechanical devices by using the Park transform to process the voltages and currents measured at the terminals of the machine. The method described can track and compensate for non-affine variations in the electrical angle $\theta_e(t)$ of the drive voltage, allowing this condition monitoring approach to work on machines connected directly to the electric utility. Both simulations and experimental results demonstrating the effectiveness of this condition monitoring method are provided. Section 2 of this paper will describe the nonidealities of the electric utility that have a direct effect on the implementation of the Park transformation, as well as the method that was used to compensate for these nonidealities. Section 3 will briefly describe the experimental platform which was used to test this condition monitoring method and then present results indicating its effectiveness. Section 4 will then conclude this paper with a review of the method which has been developed.

II. THE ADAPTIVE PARK TRANSFORM

In general, one of the difficulties inherent in describing the behavior of most rotating electric machinery is that the machine inductances are a function of both the electrical and the mechanical angles of the machine. To simplify this process, R.H. Park developed a transformation that made the analysis
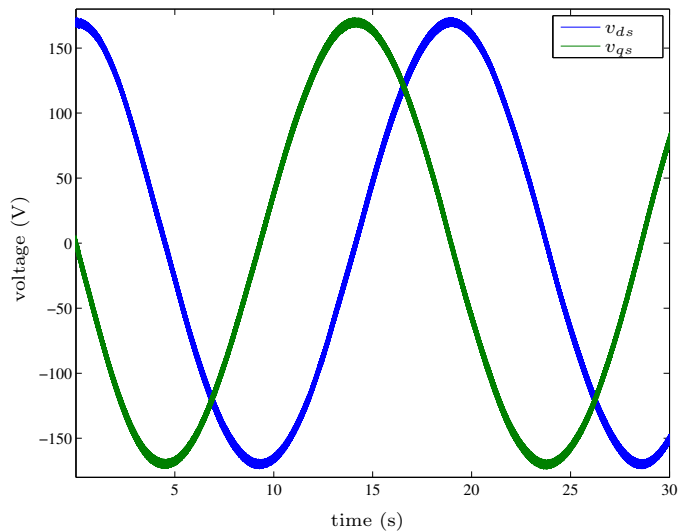

Fig. 1. v_{ds} and v_{qs} transformed without correction. The sinusoidal variation in these waveforms is due to the variation in $\phi_e(t)$.

of electric machines more straightforward by transforming the motor equations into a reference frame that is rotating synchronously with the fields in the machine [12]. This Park transformation can be written as

$$\begin{bmatrix} f_d \\ f_q \\ f_0 \end{bmatrix} = \begin{bmatrix} \cos(\theta) & \cos(\theta - 2\pi/3) & \cos(\theta + 2\pi/3) \\ -\sin(\theta) & -\sin(\theta - 2\pi/3) & -\sin(\theta + 2\pi/3) \\ 1/2 & 1/2 & 1/2 \end{bmatrix} \begin{bmatrix} f_a \\ f_b \\ f_c \end{bmatrix} \quad (1)$$

or, in a more compact form,

$$\mathbf{f_{dq0}} = \mathbf{T}(\theta)\mathbf{f_{abc}} \quad (2)$$

where f stands for the variable to be transformed, such as voltage, current, or magnetic flux. The argument of this transformation $\theta = \omega t$ can theoretically be chosen arbitrarily; one useful choice for induction machines is the electrical angle of the voltages driving the stator windings. In this case, the measured variables are transformed into the reference frame that is rotating synchronously with the driving voltages.

To implement this transformation, the angle of the electric utility θ_e must be estimated at all points in time to maintain synchronization between the transformation matrix and the observed data. Unfortunately, this angle cannot be modeled as a simple affine function of time, e.g., $\theta_e(t) = \omega_e t + \phi_e$, due to nonidealities present in the system. A more accurate functional description of the electrical angle of the utility is $\theta_e(t) = \omega_e t + \phi_e(t)$. This model for the voltage waveform on the electric utility does not capture its full harmonic content; for example, the prevalence of switching power supplies and other loads typically leads to substantial third-harmonic distortion of the utility voltage. However, the simplicity of this representation is useful, and this model will therefore be referred to extensively in this paper because it captures the effective changes in the electrical angle that occur, as well as the potential error in the estimate of the electrical frequency ω_e.

While this variation in θ_e may not be initially expected, it can be observed in experimentally measured data from the electric utility, as illustrated in Figure 1. The frequency of the utility ω_e was estimated for this waveform by fitting the first two line cycles of the data to the model of the

utility voltage $V\cos(\omega_e t + \phi_e)$, where both ω_e and ϕ_e are constant. This figure illustrates the effect of applying the Park transformation with $\theta_e(t) = \omega_e t + \phi_e$ and neglecting the variation in $\phi_e(t)$. Since v_{ds} and v_{qs} would be constant if the electrical frequency was an affine function of time, the variations apparent in this figure indicate that the estimated electrical frequency varies with time. Among other sources of distortion, neighboring load currents can induce voltages in the utility impedances that periodically distort the zero crossings or phase of the utility voltage waveform on a relatively short timescale. This experimental data suggests that this problem can indeed be formulated as a problem in which the time-varying parameter $\theta_e(t)$ must be estimated from observations of the signal $V\cos(\theta_e(t))$.

In general, the problem of identifying the argument θ_e of a sinusoidal function $v(t) = \cos(\theta_e(t))$ is highly nonlinear, as the residual between a set of observations and the output of the associated model will have a large number of local minima. These local minima can be problematic for gradient-based minimization methods, such as the Gauss-Newton or Levenberg-Marquardt algorithms, as they can cause them to converge to a parameter that is far away from the global minimum. One approach that was found to assist in avoiding the trap of local minima is described in detail in [13], and is outlined briefly below.

This solution to the problem is based upon the observation that many types of system identification problems, such as those based upon sinusoids or sums of sinusoids, have residuals that are often nearly linear in the parameters for a small subset of observations [14]. One technique for solving these nonlinear least squares problems that incorporates this observation identifies the number of datapoints for which the residual is expected to be linear, and then performs the minimization over this subset of datapoints. By solving a series of minimization problems in which the size of this subset of observations is gradually increased, the convergence of nonlinear least squares is greatly improved.

For example, suppose that one had a set of observations of a sinusoid generated by $y_{obs} = \cos(2\pi t_k)$, and that the model for this signal is $\cos(\mu t_k)$, with the resulting residual expressed as

$$r_k = \hat{y}(\mu, t_k) - y_{obs}(t_k). \tag{3}$$

Since this data is nearly linear for $t_k < 1/8$, the procedure will first identify the number of samples K for which $t_k < 1/8$. Once this length K of the subset was identified, the nonlinear least squares problem is solved using only the first K datapoints of y_{obs}, thus taking advantage of the fact that the residual of the problem is nearly linear in this region to ensure that no local minima are present. Once the final parameter estimate $\mu^{(1)}$ for this subproblem is obtained, it is then used as the initial guess to solve the next subproblem, in which the first $2K$ datapoints of y_{obs} are used to find the next parameter estimate $\mu^{(2)}$. This process continues until the number of datapoints over which the minimization takes place is equal to the number of datapoints in y_{obs}, and the parameter estimate $\mu^{\lceil (N/K) \rceil}$, which is calculated for the length of the dataset, represents the final least-squares estimate for the problem.

The advantages of this method can be seen by considering the loss function described. The normalized residual $r(\hat{\mu})/N$
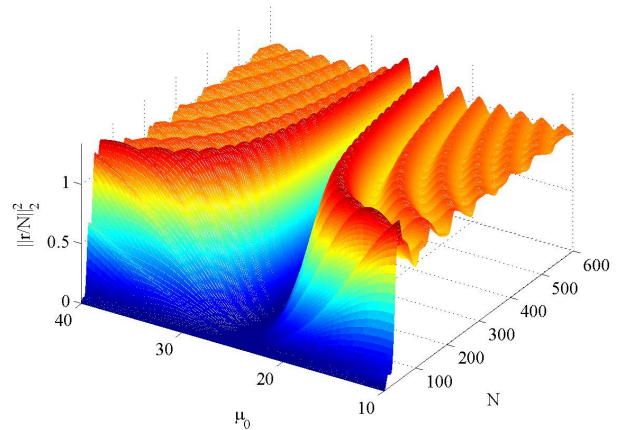

Fig. 2. Loss function showing the effect on $r(\hat{\mu})$ of varying both the initial guess $\hat{\mu}$ and the number of points K used in forming the residual.

to be minimized in this case is

$$\frac{r(\hat{\mu})}{N} = \frac{1}{N}\sum_{k=1}^{N}(\sin(\hat{\mu}kT_s) - \sin(\mu kT_s))^2 \tag{4}$$

where T_s is the sample period for the waveform, k is the sample index that runs from 1 to N, the true parameter of the system is μ, and the present estimate of the parameter is $\hat{\mu}$. Figure 2 illustrates this loss function when the number of samples of the sine wave is relatively large, so that many periods of the sine wave are represented in the data. By using the algorithm described above to find the estimate $\hat{\mu}$ by solving the series of minimization problems in which the number of samples of the observed dataset K is slowly increased from a small number to the length of the dataset N, the susceptibility of nonlinear least squares to local minima is greatly reduced.

While this approach to solving the nonlinear least squares problem has proven to be effective, it necessarily takes a long time to converge if the region over which the problem is linear is very small in comparison to the size of the dataset. An additional observation for this problem that points to a means of improving the method's performance in this regard is that one would not expect the estimate of μ to change appreciably for $t_k > 1$, and the method could presumably move very quickly through the remainder of the dataset in the absence of measurement noise. This observation can be integrated into the method by supposing that a Taylor series exists for the model, so that the residual can be rewritten

$$r_k = \overbrace{\left(\hat{y}(\mu,0) + \frac{d}{dt}\hat{y}(\mu,0)t_k + \frac{d^2}{dt^2}\hat{y}(\mu,0)t_k^2 + \cdots\right)}^{\hat{y}(\mu,t_k)} - \underbrace{\overbrace{\left(a + bt_k + ct_k^2 + \cdots\right)}}_{y_{obs}(t_k)}. \tag{5}$$

Since many problems that can be written in the above form are dominated by their DC- and first-order coefficients, it is possible to control the size of the dataset by analyzing the output of the Taylor series expansion of the residual r. The method can set the size of the increment on the dataset by comparing the coefficient of the second-order term to an established threshold, thereby ensuring that the method
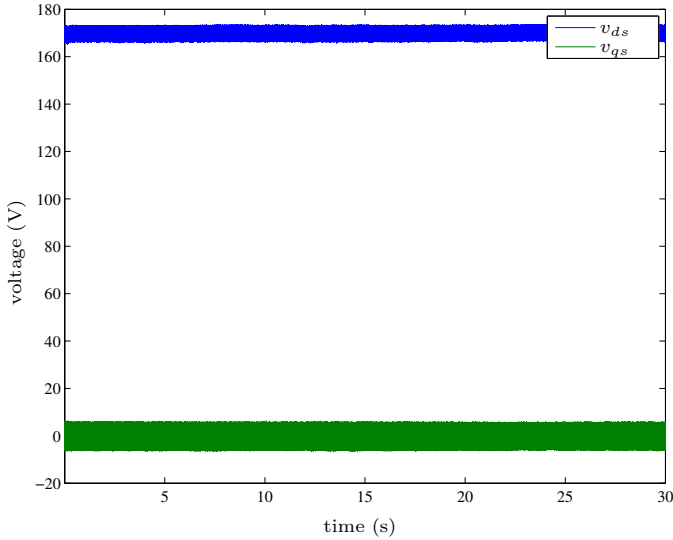
Fig. 3.   D- and Q-axis voltages transformed with phase correction.

Fig. 4.   Time-varying component of utility voltage angle.

will converge. By using the Taylor series expansion of the residual, the time that the method takes to identify the desired parameters can be improved markedly without sacrificing the ability of the method to avoid local minima. Additional details regarding the development and application of this method can be found in [13].

To compute this time-varying estimate of θ_e, it is necessary to identify the parameters V, ω_e and $\phi_e(t)$ for the observed set of balanced three-phase voltages. As all of the time-varying components of $\theta_e(t)$ can be incorporated into the term $\phi_e(t)$, the base frequency ω_e and the amplitude V of the waveform are relatively constant and can be estimated from the first two line cycles of the data. The previously described parameter identification method was then used to update the estimate of θ_e after every successive cycle, so that the time variations of ϕ_e are represented by differing successive estimates of this quantity. These updates of the phase could have been made more frequently, but laboratory experience suggested that this update frequency adequately tracked the changes in $\phi_e(t)$ over time. An additional benefit of this method for tracking the phase angle of the utility is that it does not require large amounts of data storage, as records of only a few cycles of observations must be stored at a given point in time. In addition, while it would have technically been possible to track $\theta_e(t)$ directly rather than only $\phi_e(t)$, the computational burden of re-estimating θ_e at every datapoint has minimal benefit over updating ϕ_e once every cycle.

After these estimates of ϕ_e are computed at the beginning of every line cycle, they are used to calculate θ_e at each sample point. These values are then used to implement the Park transformation from Equation 2 on the measured voltages and currents. The results obtained from implementing this transformation on experimentally measured data are discussed in the following section.

III. EXPERIMENTAL RESULTS

Initial testing of the parameter estimation method was performed in Matlab for the purposes of evaluating its performance by processing the same dataset illustrated in Figure 1. The efficacy of this method for tracking the variation in θ_e can be seen in Figure 3, as the constant nature of these waveforms suggests that the transformation was able to adequately
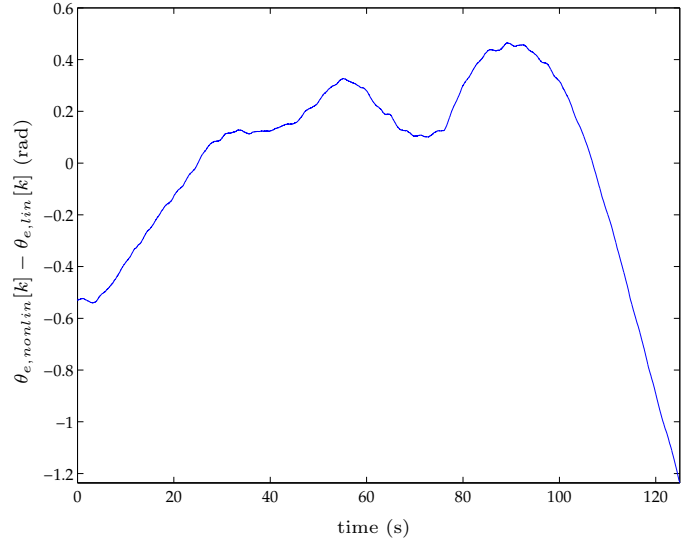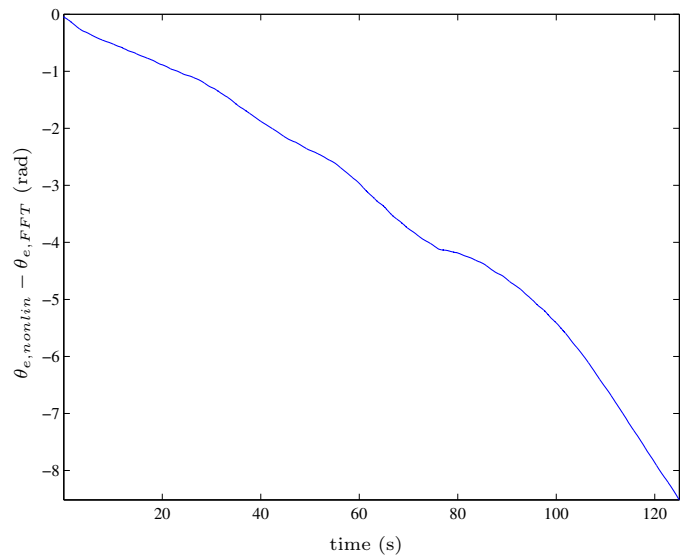

Fig. 5.   Residual between nonlinear angle estimate and FFT-based angle estimate.

compensate for the time-varying and unmodeled behavior in the observed voltage waveform. It is important to note that the angle between the voltage phases does not vary, but rather only the phase $\phi_e(t = T)$ at any instant T in comparison to the phase at time $t = 0$.

Two sets of predictions of θ_e were generated from the measured set of data used in Figures 1 and 3 to compare the measured dependence of the electrical angle of the utility with the expected electrical angle. This data was fit to the nonlinear model described in Section II, and the resulting fit is referred to as $\theta_{e,nonlin}$. Since the utility is normally modeled by $\theta_{e,lin}(t_k) = \omega_e t_k + \phi_e$, standard linear least squares techniques were used to fit this linear model to the vector $\theta_{e,nonlin}(t)$, making it possible to obtain non-time-varying estimates of the parameters ω_e and ϕ_e. The nonlinear time-varying component of the angle $\theta_e[k]$ can then be observed by forming the residual $\theta_{e,nonlin} - \theta_{e,lin}$. This is illustrated in Figure 4.

Figure 5 further illustrates the effects of the time variations in the model for the utility voltage. Rather than calculate the frequency of the utility voltage from the first two line cycles, an FFT was performed on the whole waveform, and

the peak of this FFT was used to estimate the line frequency. This has the effect of finding the average frequency over the complete waveform. This estimate of the frequency was used to fit the measured data to the usual model for the utility voltage with constant ω_e and ϕ_e, producing an estimate of the electrical angle $\theta_{e,FFT}$. Figure 5 illustrates the residual $\theta_{e,nonlin}$, obtained from the nonlinear estimation process and $\theta_{e,FFT}$. While the process of using the FFT might be expected to improve the estimate of ω_e, this plot confirms the fact that the apparent variations in θ_e should not attributed to a particular estimate of ω_e, but rather to the fact that the phase ϕ_e effectively varies with time.

A number of induction motor simulations were run to investigate the changes in i_{ds} and i_{qs} that occur during the startup transient with an increased load torque. A standard fifth-order induction motor model [6] was used to simulate the behavior of the machine. After transforming the constitutive relations into the synchronous reference frame, the following equations describe the machine behavior:

$$\frac{d\lambda_{qs}}{dt} = v_{qs} - R_s i_{qs} - \omega_e \lambda_{ds} \tag{6}$$

$$\frac{d\lambda_{ds}}{dt} = v_{ds} - R_s i_{ds} + \omega_e \lambda_{qs} \tag{7}$$

$$\frac{d\lambda_{qr}}{dt} = v_{qr} - R_r i_{qr} - (\omega_e - p\omega_r)\lambda_{dr} \tag{8}$$

$$\frac{d\lambda_{dr}}{dt} = v_{dr} - R_r i_{dr} + (\omega_e - p\omega_r)\lambda_{qr}. \tag{9}$$

where λ denotes the flux linkages with the rotor variables and parameters reflected to the stator, ω_e is the frequency of the stator excitation (i.e. the frequency the drive voltage) in rad/s, ω_r is the rotor speed in rad/s, and p is the number of pole pairs. The voltages v_{ds} and v_{qs} represent the driving voltages in this application, while v_{dr} and v_{qr} are set to zero due to the fact that the rotor bars are shorted together on a squirrel-cage machine. The flux linkages and the currents are related by the following equations:

$$\lambda_{qs} = L_{ls}i_{qs} + L_m(i_{qs} + i_{qr}) \tag{10}$$

$$\lambda_{ds} = L_{ls}i_{ds} + L_m(i_{ds} + i_{dr}) \tag{11}$$

$$\lambda_{qr} = L_{lr}i_{qr} + L_m(i_{qs} + i_{qr}) \tag{12}$$

$$\lambda_{ds} = L_{lr}i_{dr} + L_m(i_{ds} + i_{dr}). \tag{13}$$

The torque of electrical origin produced by the motor is given by

$$\tau_e = \frac{3}{2}p(\lambda_{qr}i_{dr} - \lambda_{dr}i_{qr}). \tag{14}$$

This torque τ_e is related to the mechanical load of the fan by the usual force balance equation,

$$\frac{d\omega_r}{dt} = \frac{1}{J}(\tau_e - \beta\omega_r^2). \tag{15}$$

To simulate the change in mechanical load due to the presence of liquid in the compressor cylinder, the damping coefficient β was changed between these simulations. The resulting d-axis current i_{ds} from these simulations can be seen in Figure 6. While there is initially no difference in the transient behavior of i_{ds}, there is a large difference between the two conditions after approximately 0.17 sec. This effect makes physical sense, as the load torque $\beta\omega_r^2$ is minimal while ω_r is small, so that most of the energy is accelerating the inertia of the rotor. As the rotor accelerates, the torque $\beta\omega_r$ becomes much larger, and has a substantial effect on i_{ds}.
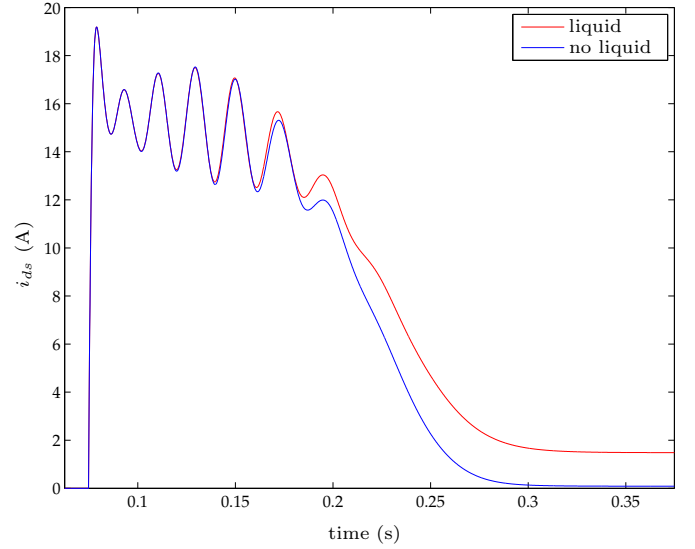

Fig. 6. Simulated i_{ds} for higher load torque in comparison to lower load torque.

Further testing of this algorithm was conducted as part of an experiment designed to study the feasibility of using this condition monitoring method to detect changes in the mechanical loading on the pistons of a 3/4 HP refrigeration compressor due to the presence of liquid in the cylinders. A set of three LEM LA-55P current transducers and three LEM LV-25P voltage transducers were installed on the compressor and used to measure the voltages and currents at the motor terminals. These sensors were interfaced to an 8 channel custom data acquisition system that operated at a sampling rate of 8 kHz/channel, and a Debian Linux-based PC was used to acquire the data.

Two sets of data were collected with this experimental setup to verify the behavior that was observed in the simulated results. The first of these datasets was collected under normal conditions, while the second set was collected when there was liquid refrigerant present in the compressor cylinder. Care was taken during these experiments to ensure that the compressor started from identical conditions (i.e. piston position and winding temperature) for each dataset. Figure 7 shows the two sets of traces corresponding to the compressor starts with and without the presence of liquid in the compressor cylinder.

These results demonstrate the effectiveness of electrically-based methods for the identification of liquid refrigerant in the compressor cylinder. It is particularly notable that there is considerable qualitative agreement between the shapes of the simulated i_{ds} and the experimentally observed i_{ds} in that the effect of the liquid on i_{ds} is manifested predominantly at the end of the transient. The similarity of the steady state values of i_{ds} can be attributed to the fact that no liquid is present in the cylinder after it is ejected, causing i_{ds} for this case to be identical to i_{ds} when no liquid was ever present in the cylinder. A condition monitoring method to identify the presence of liquid could thus be constructed by analyzing the interval between 0.6 and 0.12 sec to distinguish between faulty and non-faulty behavior. This figure shows very clear differences between the two sets of traces corresponding to compressor starts in normal operating conditions and under faulty operating conditions, suggesting that this condition monitoring method would be useful for identifying this mechanical fault using
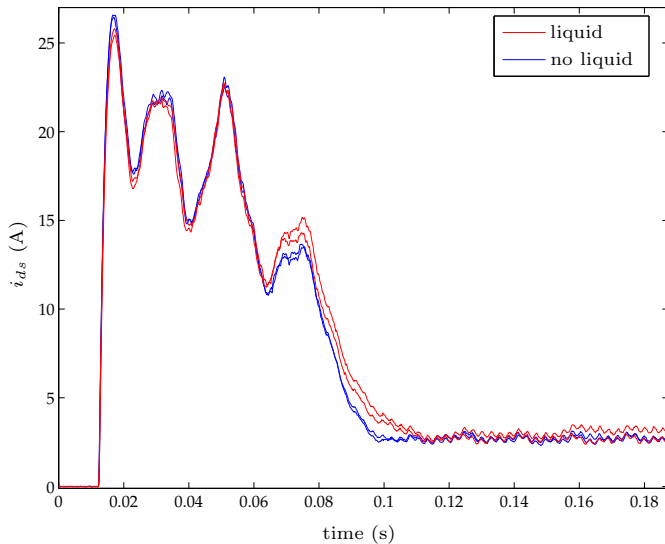
Fig. 7. i_{ds} during transient slugging for 2 tests with liquid in the cylinder in comparison to 2 tests without liquid in the cylinder.

only observations of electrical variables. Additional related results and development of this condition monitoring method can be found in [7].

IV. DISCUSSION

This paper described a method for preprocessing observed three-phase current data from electromechanical systems that could be used for condition monitoring that is invariant to both changes in the initial electrical angle and to variations in the electrical angle with time. This method was demonstrated to be effective both on a simulation of an induction machine and also on an experimental refrigeration compressor connected directly to the utility.

ACKNOWLEDGMENTS

REFERENCES

[1] M. Benbouzid. A review of induction motors signature analysis as a medium for faults detection. *IEEE Transactions on Industrial Electronics*, 47(5):984–993, October 2000.

[2] S. Cruz, A. Cardoso, and H. Toliyat. Diagnosis of stator, rotor, and airgap eccentricity faults in three-phase induction motors based on the multiple reference frames theory. In *2003 Industry Applications Conference*, volume 2, pages 1340–1346, October 2003.

[3] K. Hurst and T. Habetler. Sensorless speed measurement using current harmonic spectral estimation in induction motor drives. *IEEE Transactions on Power Electronics*, 11(1):1, January 1996.

[4] J.-H. Jung, L. J-J., and K. B-H. Online diagnosis of induction motors using mcsa. *IEEE Transactions on Industrial Electronics*, 53(6):1842–1852, December 2006.

[5] K. Kim, A. Parlos, and R. Baharadwaj. Sensorless fault diagnosis of induction motors. *IEEE Transactions on Industrial Electronics*, 50(5):1038–1051, October 2003.

[6] P. Krause, O. Wasynczuk, and S. Sudhoff. *Analysis of Electric Machinery*. McGraw-Hill, 1986.

[7] C. Laughman. *Fault Detection Methods for Vapor-Compression Air Conditioners Using Electrical Measurements*. PhD thesis, M.I.T., 2008.

[8] C. Laughman, K. Lee, R. Cox, S. Shaw, S. Leeb, L. Norford, and P. Armstrong. Power signature analysis. *IEEE Power and Energy Magazine*, 1(2):56–63, Mar. 2003.

[9] C. Laughman, S. Leeb, L. Norford, S. Shaw, and P. Armstrong. A two-step method for estimating the parameters of induction machine models. In *Proceedings of the 2009 Energy Conversion Congress and Exposition*, pages 262–269, 2009.

[10] S. Leeb, S. Shaw, and J. Kirtley. Transient event detection in spectral envelope estimates for nonintrusive load monitoring. *IEEE Transactions in Power Delivery*, 10(3):1200–1210, July 1995.

[11] S. Nandi, H. Toliyat, and X. Li. Condition monitoring and diagnosis of electrical motors - a review. *IEEE Transactions on Energy Conversion*, 20(4):719–729, December 2005.

[12] R. Park. Two-reaction theory of synchronous machines: Generalized method of analysis, part i. *Transactions of the AIEE*, 48:716–727, 1929.

[13] S. Shaw and C. Laughman. A method for nonlinear least squares using structured residuals. *IEEE Transactions on Automatic Control*, 51(10):1704–1708, Oct. 2006.

[14] S. Shaw and S. Leeb. Identification of induction motor parameters from transient stator current measurements. *IEEE Transactions on Industrial Electronics*, 46(1):139–149, Feb. 1999.

[15] A. Siddique and B. Singh. A review of stator fault monitoring techniques of induction motors. *IEEE Transactions on Energy Conversion*, 20(1):106–114, March 2005.

[16] R. Tallam, S. Lee, G. Stone, G. Kliman, J. Yoo, T. Habetler, and R. Harley. A survey of methods for detection of stator-related faults in induction machines. *IEEE Transactions on Industry Applications*, 43(4):920–933, July-August 2007.

[17] P. Tavner. Review of condition monitoring of electrical machines. *IET Electric Power Applications*, 2(4):215–247, 2008.